Blocking Stemness and Metastatic Properties of Ovarian Cancer Cells by Targeting p70S6K with Dendrimer Nanovector-Based siRNA Delivery

Jing Ma, Shashwati Kala, Susan Yung, Tak Mao Chan, Yu Cao, Yifan Jiang, Xiaoxuan Liu, Suzanne Giorgio, Ling Peng, Alice Wong

Blocking stemness and metastatic properties of ovarian cancer cells by targeting $p70^{S6K}$ with dendrimer nanovector-based siRNA delivery

Jing Ma[1], Shashwati Kala[1], Susan Yung[2], Tak Mao Chan[2], Yu Cao[3], Yifan Jiang[3], Xiaoxuan Liu[4], Suzanne Giorgio[3], Ling Peng[3], and Alice ST Wong[1]

[1]School of Biological Sciences, University of Hong Kong, Pokfulam Road, Hong Kong

[2]Department of Medicine, University of Hong Kong, Sassoon Road, Hong Kong

[3]Aix-Marseille Université, CNRS, Centre Interdisciplinaire de Nanoscience de Marseille, UMR 7325, « Equipe Labellisée Ligue Contre le Cancer », 13288 Marseille, France

[4]State Key Laboratory of Natural Medicines and Jiangsu Key Laboratory of Drug Discovery for Metabolic Diseases, Center of Drug Discovery, China Pharmaceutical University, 210009 Nanjing, China

Correspondence: Alice ST Wong. Email: awong1@hku.hk

Ling Peng. Email: ling.peng@univ-amu.fr

Running title: Target cancer stem cells by siRNA nanoparticles

Keywords: cancer stem cells, siRNA delivery, dendrimer nanovector

Abstract

Metastasis is the cause of most (>90%) cancer deaths, and current treatments have not proven to be effective. Approaches to understanding the biological process, unraveling the most effective molecular target(s), and implementing nanotechnology to increase the therapeutic index are expected to facilitate cancer therapy against metastasis. Here, we demonstrate the potential advantages of bringing these three approaches together through the rational design of a siRNA that targets $p70^{S6K}$ in cancer stem cells (CSCs) in combination with dendrimer nanotechnology-based siRNA delivery. Our results demonstrated that the generation 6 (G_6) poly(amidoamine) dendrimer can be used as a nanovector to effectively deliver $p70^{S6K}$ siRNA by forming uniform dendriplex nanoparticles which protect the siRNA from degradation. These nanoparticles were able to significantly knockdown $p70^{S6K}$ in ovarian CSCs, leading to a marked reduction in CSC proliferation and expansion without obvious toxicity towards normal ovarian surface epithelial cells. Furthermore, treatment with the $p70^{S6K}$ siRNA/G_6 dendriplexes substantially decreased mesothelial interaction, migration and invasion of CSCs *in vitro* as well as tumor growth and metastasis in CSC xenograft mice *in vivo*. Collectively, these results suggest that $p70^{S6K}$ constitutes a promising therapeutic target, and the use of siRNA in combination with nanotechnology-based delivery may constitute a new approach for molecularly targeted cancer therapy to treat metastasis.

Introduction

Metastasis accounts for the majority (>90%) of cancer deaths, yet aggressive treatment has not proven to be effective in improving the survival rate of the cancer patients in the past several decades[1,2]. Three emerging approaches will drive the development of novel and effective treatments to facilitate cancer therapy. The first is the ability to correctly target the metastatic lesion, leading to increased antitumor efficacy. The second is the unraveling of the oncogenic drivers to facilitate development of the most effective molecularly targeted therapy. The third is the use of nanotechnology that selectively targets these drivers to enhance the therapeutic index. However, despite advances in each of these areas, the interaction of all three is urgently needed to improve therapeutic outcomes.

Ovarian cancer is a highly metastatic cancer, with most (>70%) patients being diagnosed at an advanced/metastatic stage (stages III and IV)[3]. Consequently, it constitutes an excellent model for identifying the mechanisms required for metastasis. One recent discovery that has revolutionized our view of tumor progression is the existence of cancer stem cells and/or tumor-initiating cells (jointly known as CSCs)[4]. In contrast to bulk tumor cells, CSCs are the key driving force not only for tumor development, but also for initiating metastasis and recurrence[5]. Cancer cells possess a stem-like gene signature that correlates with poor progression-free and overall survival in cancer patients. The existence of these CSCs may well explain clinical observations about the metastatic cascade and early metastasis[6,7]. As such, strategies aiming to eradicate CSCs represent rational approaches for cancer treatment[8].

Protein kinases are the favored class of targets for drug development, in particular for cancer treatment. p70 S6 kinase ($p70^{S6K}$), an effector of the phosphatidylinositol 3-kinase/Akt pathway, is of interest because it is frequently activated in ovarian cancer[9].

We recently published data describing for the first time that $p70^{S6K}$ plays a key role in tumor progression, particularly metastasis[10-13]. Constitutive activation of $p70^{S6K}$ is increased in ovarian carcinomas as compared to benign or borderline lesions, and this activation correlates with high tumor grade and aggressive malignant phenotype[11]. The findings that $p70^{S6K}$ is involved in different mechanisms that promote the metastatic growth of ovarian tumor cells, such as cell adhesion, migration and matrix degradation, suggest that it could be a promising target for developing novel therapeutics against ovarian cancer. However, the role of $p70^{S6K}$ in inducing a stem-like phenotype, which is a key process directly linked to tumor aggressiveness, has not been established. Additionally, $p70^{S6K}$ is a downstream effector of mTOR, and can be inhibited by small molecular inhibitors of mTOR such as rapamycin and its derivatives. Some of these inhibitors have recently been employed in various clinical trials, but most of them have limited clinical use because they lack specificity, exhibit poor pharmacologic properties and cause potentially adverse side effects[14,15].

RNA interference (RNAi)-based gene silencing technology, which uses small interfering RNAs (siRNAs) to break down the target mRNA in a sequence-specific manner, holds great promise for targeting disease-associated genes. It is broadly, yet specifically, applicable to any gene with known sequence. It is particularly advantageous for silencing "undruggable" genes or therapeutic targets which are difficult to target, for example, protein kinases. In addition, RNAi offers unique benefits such as superior specificity and efficiency, yet it is a quick and affordable approach when compared to small molecular inhibitors[16]. Unlike small molecule inhibitors which are often hydrophobic and can readily enter into cells, siRNAs are negatively charged and cannot easily cross the plasma membrane. Moreover, naked siRNA is highly unstable (half-life ~ 3 mins). Consequently, RNAi-based therapeutic application

requires safe and effective siRNA delivery systems, which can mask the negative charge of the siRNA, protect the siRNA from degradation and deliver it safely to the site of interest.

Both viral and nonviral delivery systems have been explored for siRNA delivery. Although viral delivery is very effective, the immunogenicity and toxicity of viral vectors in humans at therapeutic doses has prompted the urgent development of nonviral alternatives[17]. Lipids and polymers are the most commonly used nonviral vectors for siRNA delivery[18-20]. Cationic dendrimers, a special family of synthetic polymer, are showing great promise for siRNA delivery because dendrimers have a well-defined molecular architecture, precisely controlled chemical structure and unique multivalent properties confined with a small nanosized volume[21]. Recently, we reported that structurally flexible poly(amidoamine) PAMAM dendrimers are particularly effective for delivering siRNA[22,23]. These PAMAM dendrimers bear triethanolamine (TEA) as an extended core at the center, primary amines on the surface and tertiary amines at the branch sites (Figure 1A)[24]. They are positively charged under physiological conditions and can assemble with the negatively charged siRNA via electrostatic interactions to form nanosized dendriplexes, which effectively protect the siRNA from degradation while also masking the high negative charge of the siRNA (Figure 1B).[23-29] These complexes also prolong the half-life of the siRNA in plasma and enhance accumulation of the siRNA specifically at tumor lesions via the Enhanced Permeation and Retention (EPR) effect.[30-32] The EPR effect is the property by which nanosized particles (typically from 10 to 200 nm) tend to accumulate in tumor tissue much more than they do in normal tissues.[33-34] This is because rapidly growing tumor cells aggregate in a confined space, and are surrounded by defective endothelial cells with wide fenestrations. In addition, tumor tissues show increased retention of

nanoparticles because they usually lack effective lymphatic drainage, which would filter out nanosized particles under normal conditions. Thus, the EPR effect helps to carry the nanoparticles into, and spread them inside, the tumor tissue, a process which is also known as passive tumor targeting. As a result, the EPR effect is important for nanoparticle delivery to and accumulation within tumor lesion, promoting uptake into cancer cells. After internalization, the siRNA will be dissociated from the dendriplexes via the proton sponge effect,[22] and will then engage with the RNAi machinery for potent gene silencing (Figure 1B).

Here we demonstrate for the first time that the generation 6 (G_6) TEA-core PAMAM dendrimer forms stable dendriplexes with a $p70^{S6K}$ siRNA for targeting ovarian CSCs. The formed $p70^{S6K}$ siRNA/G_6 dendriplexes can protect $p70^{S6K}$ siRNA from RNase A digestion and effectively knock down $p70^{S6K}$ protein expression in ovarian CSCs. We also provide evidence that $p70^{S6K}$ siRNA/G_6 dendriplexes can inhibit ovarian CSC expansion, adhesion, and migration/invasion, all of which are key processes in the metastatic cascade. Furthermore, treatment with the $p70^{S6K}$ siRNA/G_6 dendriplexes led to significant inhibition of ovarian tumor growth and effective regression of metastasis in CSC xenograft mice. Altogether, our results suggest that combining siRNA therapeutics with dendrimer nanotechnology-based delivery to target $p70^{S6K}$ in CSCs may constitute a new means for molecularly targeted therapy to treat cancer metastasis.

Results

G_6 forms stable dendriplexes with $p70^{S6K}$ siRNA and protects it from degradation

The TEA-core PAMAM dendrimer G_6 has primary amines on the surface and is hence positively charged under physiological conditions. It is therefore capable of

compacting the negatively charged siRNA into dendriplexes via electrostatic interactions. The formation of $p70^{S6K}$ siRNA/G_6 dendriplexes was assessed using gel mobility shift assays by varying the N/P ratio, a value which denotes the total number of dendrimer amine terminals versus the total number of siRNA phosphates. As displayed in Figure 2A, $p70^{S6K}$ siRNA showed significantly retarded migration in the presence of G_6 at an N/P ratio of 2.5 or above, indicating the formation of stable siRNA/G_6 dendriplexes. Transmission electronic microscopy (TEM) imaging further revealed small, uniform, spherical siRNA/G_6 dendriplexes (Figure 2B). Dynamic light scattering (DLS) analysis also confirmed that the siRNA/G_6 dendriplexes had an average size of ~ 30 nm and polydispersity of 0.239 (Figure 2C). The zeta potential was + 25.8 mV at an N/P ratio of 10 (Figure 2C). The small size and positive zeta potential of the $p70^{S6K}$ siRNA/G_6 dendriplexes are two advantageous characteristics for promoting cellular uptake. The zeta potential value, of around 20 mV, also indicates the stable colloidal property of the dendriplexes. Indeed, G_6 effectively protected siRNA from enzymatic digestion by RNase A, whereas free siRNA was degraded rapidly within 5 minutes upon treatment with RNase A (Figure 2D). Collectively, our findings affirmed the formation of stable siRNA/G_6 dendriplexes.

$p70^{S6K}$ siRNA/G_6 dendriplexes effectively silence $p70^{S6K}$ protein expression and inhibit CSC proliferation

We next assessed the ability of $p70^{S6K}$ siRNA/G_6 dendriplexes to down-regulate $p70^{S6K}$ protein in ovarian CSCs. CSCs were successfully isolated from ovarian cancer cell lines and cancerous ovarian tissues using a strategy based on the ability of CSCs to self-renew and grow as spheres or sphere-forming cells under non-adherent conditions which select stem cells and closely mimic the malignant ascites in the advanced stages

of ovarian carcinoma[35]. In addition to the sphere-forming properties of CSCs, we also assessed the stemness markers Oct4, c-Kit (CD117), Nanog, and Bmi-1,[33] and we affirmed the *in vivo* tumorigenic potential of these cells by showing that as few as 100 CSCs, when injected subcutaneously in athymic nude mice, gave consistent and full recapitulation of the original tumor[35]. These CSC-derived tumors were capable of serial transplantation and were similar in histopathology to human ovarian cancer[35]. There was also a significant increase in the CA125 tumor antigen, which is the gold standard tumor marker of ovarian carcinomas, in CSC lysates[35]. When 10% fetal bovine serum was added to induce differentiation, the CSCs adhered and formed symmetric holoclones. Moreover, the differentiated cells had reduced expression of the stemness markers Oct4, c-Kit (CD117), Nanog, and Bmi-1 compared to CSCs[35]. This provides further evidence of the undifferentiated phenotype of the CSCs.

CSCs obtained using the selection strategy described above were treated with $p70^{S6K}$ siRNA/G_6 dendriplexes and allowed to form spheres in non-adherent, stem-cell selective conditions. Remarkably, $p70^{S6K}$ siRNA/G_6 dendriplexes were able to knock down $p70^{S6K}$ protein expression in a concentration-dependent manner, with about 90% gene silencing achieved at 50 nM siRNA, whereas no down-regulation of $p70^{S6K}$ was observed with nonspecific (NS) siRNA/G_6 dendriplexes (Figure 3A). Neither G_6 alone nor naked siRNA alone had any notable effect (Figure 3B). Further MTT analysis revealed that $p70^{S6K}$ siRNA/G_6 dendriplexes were able to inhibit more than 50% of the cell proliferation as compared to NS siRNA/G_6 dendriplexes, whereas no inhibition was observed with G_6 alone or naked siRNA (Figure 3C). In addition, treating SKOV-3 non-CSCs with $p70^{S6K}$ siRNA/G_6 dendriplexes also resulted in significant downregulation of $p70^{S6K}$ protein (Figure 3D), leading to potent inhibition of cell growth (Figure 3E). These results are consistent with the reported observations of the effect of $p70^{S6K}$ on

tumor growth inhibition [36] and suggest that targeting $p70^{S6K}$ may lead to a more pronounced and durable anticancer effect. Similar experiments with HEYA8 CSCs revealed inhibition on $p70^{S6K}$ expression (Figure 3F) and cell growth (Figure 3G) that was indistinguishable from that in SKOV-3 CSCs. It is notable that $p70^{S6K}$ siRNA/G_6 dendriplexes did not affect the growth of normal ovarian surface epithelial (OSE) cells (Figure 3H). These results suggest that suppression of $p70^{S6K}$ can inhibit ovarian neoplastic processes.

$p70^{S6K}$ siRNA/G_6 dendriplexes inhibit stemness and regrowth (relapse) of CSCs

Unlike their non-CSC counterparts, ovarian CSCs express the stem cell markers Bmi-1, Nanog, and Oct4. Under sphere-forming conditions, we showed that $p70^{S6K}$ siRNA/G_6 dendriplexes, but not NS siRNA/G_6 dendriplexes, depleted all these stem cell markers of ovarian CSCs (Figure 4A). This highlights that down-regulation of $p70^{S6K}$ inhibits the stemness of CSCs.

The sphere-forming ability of CSCs after serial passage is another indirect hallmark of stem cell renewal. We therefore further determined the effect of $p70^{S6K}$ knockdown in a relapse experiment by dissociating CSCs and reseeding the cells to test their ability to develop secondary spheres in the presence of NS siRNA/G_6 and $p70^{S6K}$ siRNA/G_6 dendriplexes. Daily imaging showed that the NS siRNA/G_6 dendriplexes had no effect at all, and secondary tumor spheres started to form on day 3, similar to the non-treatment control (Figure 4B). In contrast, no secondary spheres were formed, even after 7 days, by the CSCs treated with $p70^{S6K}$ siRNA/G_6 dendriplexes (Figure 4B). These results indicate that $p70^{S6K}$ is functionally important for the stemness of CSCs, and that inhibition of $p70^{S6K}$ effectively blocks self-renewal of CSCs.

p70^{S6K} siRNA/G$_6$ dendriplexes inhibit CSC adhesion, migration and invasion

Ovarian cancer metastasis often occurs from exfoliation into ascites, attachment to the peritoneal mesothelium, and then migration/invasion into the local stroma[37]. Therefore, successful adhesion to the peritoneal mesothelium is the first key step in ovarian cancer metastasis[38], and strong cell adhesion will promote CSC seeding and growth as a precursor to metastasis. Consequently, inhibition of CSC adhesion should attenuate metastasis. We therefore assessed p70^{S6K} siRNA/G$_6$ dendriplexes for their effect on cell adhesion using a fluorescent-based coculture assay to monitor the interactions between CSCs and primary human mesothelial cells. CSCs transfected with siRNA dendriplexes were fluorescently labeled, overlaid onto a monolayer of confluent primary human mesothelial cells and allowed to attach for 30 min. The non-adherent CSCs were removed, and the adherent spheres were fixed and counted (Figure 5A). CSCs treated with p70^{S6K} siRNA/G$_6$ dendriplexes showed substantially decreased adhesion to mesothelial cells compared to those treated with NS siRNA/G$_6$ dendriplexes (90% inhibition; $P < 0.0001$) (Figure 5A). This demonstrates that the down-regulation of p70^{S6K} led to the effective inhibition of CSC adhesion.

Cell migration and invasion are two key processes that directly contribute to metastasis. Active migration of tumor cells is a prerequisite for tumor cell dissemination, whereas invasive properties allow tumor cells to extend into and penetrate the surrounding tissues. Once ovarian tumor cells have adhered to the peritoneal mesothelium, they can migrate and invade into the peritoneal surface. The surface of the peritoneum consists of stromal cells and the extracellular matrix, which contains collagen type I, fibronectin, vitronectin and a continuous basement membrane including laminin and collagen type IV[37]. To further investigate the physiological importance of p70^{S6K} in metastatic signaling, we explored whether p70^{S6K} regulates cell

migration and invasion using ovarian CSCs seeded in non-coated and Matrigel-coated transwells, respectively. Matrigel is often used as a biomimetic ECM substrate. As shown in Figure 5B and 5C, NS siRNA/G_6 dendriplexes had no effect on the migration or invasion of CSCs, while $p70^{S6K}$ siRNA/G_6 dendriplexes significantly inhibited the ability of CSCs to migrate and invade through the filter (migration: 66.67 ± 7.37% inhibition; invasion: 74.03 ± 10.41% inhibition). Collectively, these results demonstrate that $p70^{S6K}$ suppression effectively impedes CSC migration and invasion.

$p70^{S6K}$ siRNA/G_6 dendriplexes inhibit tumor growth in a CSC xenograft model

To further illustrate the role of the $p70^{S6K}$ siRNA/G_6 dendriplexes *in vivo*, we used SKOV-3 CSCs in a mouse xenograft model of ovarian cancer. We first examined whether the siRNA/G_6 dendriplexes could effectively reach the tumor site via EPR effect as the nanosized particles tend to accumulate much more in tumor lesions than normal tissues.[30,31,33,34] We used a fluorescent dye Cy5 labeled siRNA to perform the biodistribution profile of the siRNA/G_6 dendriplexes in the CSC-xenograft mice. As we can see in Figure 6, strong and characteristic Cy5 fluorescent signal was cumulated at the tumor site, peaked at 1 h and retained for 24 h (Figure 6A) than normal tissue (Figure 6B). This finding highlights the successful accumulation of the siRNA/dendrimer complexes at tumor site via the beneficial and powerful EPR effect.

We then assessed tumor growth in CSC-xenograft mice following the silencing of the $p70^{S6K}$. Compared with NS siRNA/G_6 dendriplexes, the $p70^{S6K}$ siRNA/G_6 dendriplexes effectively inhibited tumor growth (Figure 7A and B). One week after the first dendriplex injection, the tumor volume in mice treated with the $p70^{S6K}$ siRNA/G_6 dendriplexes was only 6.9 % of that in mice treated with the NS siRNA/G_6 dendriplexes, and the levels of $p70^{S6K}$ and Ki67 in tumors were significantly decreased to 17% and

16%, respectively, of the levels in controls as revealed by the immunohistochemistry (IHC) analysis (Figure 7C). We also used western blotting to assess the protein level of $p70^{S6K}$ in tumor tissues (Figure 7D), which perfectly matched the IHC data. In addition, there was considerable down-regulation of expression of the stem cell markers Bmi-1, Nanog and Oct4 in tumors from the groups treated with $p70^{S6K}$ siRNA/G_6 dendriplexes compared to the group treated with NS siRNA/G_6 dendriplexes (Figure 7E), indicating that the CSC stemness was indeed inhibited following the silencing of $p70^{S6K}$. Also, there was a significant down-regulation of expression of stem cell marker CD133 in $p70^{S6K}$ siRNA/G_6 dendriplexes group as compared to NS siRNA/G_6 dendriplexes group (Figure 7F), further affirming the inhibition of CSC stemness. All these results attest that $p70^{S6K}$ siRNA/G_6 dendriplexes were potent in silencing $p70^{S6K}$, hence inhibiting the CSC stemness and retarding the tumor growth in SKOV-3 CSCs xenografts.

As the siRNA/dendrimer complex showed considerable uptake in liver, we hence checked the liver and the blood biochemistry by measuring the alanine transaminase (ALT) and aspartate aminotransferase (AST) level in the mice blood. There was no significant difference between the mice treated with the NS siRNA/G_6 or the siRNA/G_6 dendriplexes (Figure 7H and 7I). In addition, no sign of abnormal behavior of the mice was observed, neither was the body weight (Figure 7G). These results suggest that the siRNA/G_6 dendriplexes exhibited no evident acute toxicity.

$p70^{S6K}$ siRNA/G_6 dendriplexes inhibit metastasis in a CSC xenograft model

To further demonstrate the suppression of $p70^{S6K}$ to inhibit metastasis of ovarian cancer, we used a metastatic ovarian cancer model using CSC cells. The $p70^{S6K}$ siRNA/G_6 dendriplexes considerably inhibited tumor metastasis compared with NS siRNA/G_6 dendriplexes. Upon three week's treatment, the tumor number in mice

treated with the $p70^{S6K}$ siRNA/G_6 dendriplexes was only 12.92 % of that in mice treated with the NS siRNA/G_6 dendriplexes (Figure 8A and 8B), demonstrating the effective inhibition of metastasis. Also, the ascites volume in mice treated with $p70^{S6K}$ siRNA/G_6 dendriplexes was only 5.77% of that in mice treated with NS siRNA/G_6 dendriplexes (Figure 8C)**.** After three weeks, only two mice survived in the group treated with NS siRNA/G_6 dendriplexes (Figure 8D), whereas the mice treated with $p70^{S6K}$ siRNA/G_6 dendriplexes were all alive, healthy and behaved normally. Collectively, our results indicate that the siRNA/G_6 dendriplexes exhibited excellent potency against tumor growth and metastasis, yet without any evident acute toxicity.

Discussion

Metastasis is a major problem for cancer treatment, and CSCs are critical for tumor maintenance, metastasis, and resistance to therapy. Effective targeting of CSCs is therefore of fundamental importance for the development of novel cancer therapy. By eradicating CSCs or residual tumor-initiating cells, it should be possible to treat metastasis and completely cure cancer. Here, for the first time, we provide evidence that $p70^{S6K}$, a key intracellular signaling mediator of multiple growth factors which is frequently activated in ovarian cancer, plays a critical role in the expansion and subsequent adhesion, migration and invasion of CSCs - each contributing to metastasis. We show in this work that a siRNA targeting $p70^{S6K}$ siRNA can be delivered to ovarian CSCs using the dendrimer nanovector G_6. The $p70^{S6K}$ siRNA/G_6 dendriplex nanoparticles effectively knock down $p70^{S6K}$ protein expression, leading to potent inhibition of ovarian CSC expansion, adhesion and migration/invasion *in vitro*, as well as inhibition of tumor growth and metastasis in CSC xenograft mice. Our studies demonstrate that $p70^{S6K}$ siRNA delivered by the dendrimer nanovector has the potential

to inhibit ovarian cancer metastasis by targeting the stemness of ovarian cancer cells.

The data presented here, together with our previous studies[10-13], indicate that $p70^{S6K}$ may act at many levels to increase the metastatic potential and aggressive behavior that are characteristic of ovarian cancer. We report here that $p70^{S6K}$, which has a well-established role in protein synthesis, is involved in the regulation of stem cell marker genes, as revealed by RT-PCR. Therefore, this response is apparently regulated at the transcriptional level. Currently, it is unclear how $p70^{S6K}$ regulates gene transcription, but there is increasing evidence that $p70^{S6K}$ can migrate into the nucleus in response to various stimuli[39-41] and some $p70^{S6K}$ substrates, such as CREM and TRAF-4, are resident in the nucleus[42-43]. Whether these transcription factors participate in the $p70^{S6K}$–mediated activation of stem cell marker genes remains to be determined. Nevertheless, the involvement of $p70^{S6K}$ in CSC multicellular spheroid formation, adhesion to mesothelial cells, and migration/invasion suggest that it could be an attractive target for effective treatment of metastatic ovarian cancer. Our findings are particularly relevant to the large number of ovarian carcinomas which constitutively express $p70^{S6K}$ at higher levels than normal tissues, and are associated with lower survival and worse outcomes for patients[11]. Moreover, $p70^{S6K}$ is also activated in colon, liver, and breast cancers in addition to ovarian cancer. Therefore, our strategy using siRNA that specifically targets $p70^{S6K}$ in CSCs will have broader relevance to a range of other cancers.

siRNA-based gene silencing is widely expected to bring new hope for cancer therapy by specifically and effectively blocking genes involved in malignancy, especially those which are otherwise difficult to target. Nevertheless, successful implementation of siRNA therapeutics requires safe and effective delivery systems to protect the siRNA from degradation and mask its high negative charge for cell

membrane penetration and effective delivery. We have previously developed structurally flexible TEA-core PAMAM dendrimers as safe and effective nanovectors for siRNA delivery and gene silencing[22-29]. These dendrimers are able to compact siRNA into small and uniform nanoparticles which protect siRNA from degradation and promote cell uptake. The open, flexible structure of the dendrimer allows water molecules to penetrate the interior more easily, which improves the efficiency of delivery by leading to more efficient release of the cargo molecules[44]. In this work, we have shown that the TEA-core PAMAM dendrimer of generation 6 (G_6) forms stable nanoparticles with $p70^{S6K}$ siRNA, protecting $p70^{S6K}$ siRNA from RNase A digestion and effectively delivering the siRNA into ovarian CSCs to knock down $p70^{S6K}$ protein expression. This leads to a marked reduction in CSC proliferation, expansion, adhesion and migration/invasion, without obvious toxicity towards normal OSE cells. Compared to our earlier experiments using a commercially available transfection agent (siLectFect) for siRNA delivery[10-13], the PAMAM dendrimer applied in this work can deliver a similar gene silencing effect using the same amount of siRNA. This further proves that the dendrimer delivery system is highly effective in initiating siRNA-based applications. In addition, effective inhibition and regression of CSC xenograft tumors was achieved upon treatment with the $p70^{S6K}$ siRNA/G_6 dendriplexes. The effective *in vivo* activity observed in our study can be ascribed to the EPR effect in combination with the excellent siRNA delivery capacity of our dendrimer. These results further confirm and validate the excellent performance of our structurally flexible PAMAM dendrimers for siRNA delivery and their promising potential in translation of siRNA therapeutics for future clinical applications.[22]

Altogether, our findings presented in this study are also of clinical significance because ovarian cancer is particularly aggressive and no current therapies are effective.

Ovarian cancer, in particular the metastatic ovarian cancer form, has the highest mortality rate of all gynecological tumors. The prognosis is poor, and the 5-year survival rate is <25%. Although chemotherapy is the most commonly used treatment, it has not proven to be effective in improving the survival of ovarian cancer patients in the past several decades. In addition, the distressing and debilitating side effects of chemotherapy significantly impact quality of life. It is also worth mentioning that a Phase I/II clinical trial of a dendritic cell vaccine with mRNA from CSCs has been recently carried out in ovarian cancer patients, but there was no increase in median survival time for either platinum-sensitive or platinum-resistant cases in combination with or without chemotherapy[45]. Therefore, there is a great need for the development of new and effective therapeutic strategies to treat ovarian cancer successfully. We have shown here that dendriplex nanoparticles containing $p70^{S6K}$ siRNA can specifically reduce the stemness and metastatic properties of ovarian CSCs. This constitutes a promising approach for molecularly targeted therapy to treat ovarian cancer metastasis. Since $p70^{S6K}$ is also activated in several other cancers, our approach using siRNA targeting of $p70^{S6K}$ in CSCs will have wide implications for fighting against life-threatening cancers in general. We are actively working in this direction.

Materials and Methods

Dendrimer/siRNA complexation

Generations 6 TEA-core PAMAM dendrimer (M_W=43648 g/mol, 192 amine end groups) was used in this study. The G_6 dendrimer was dissolved in MQ water to 20 μM. $p70^{S6K}$ siRNA (5'-GACAAAAUCCUCAAAUGUA-3') and nonspecific siRNA (5'-GGCTACGTCCAGGAGCGCA-3') were obtained from Dharmacon (Lafayette, CO). The N/P ratio and siRNA dendriplexes were prepared as described[25]. To demonstrate

the formation of siRNA dendriplexes, agarose gel retardation assay was used. siRNA dendriplexes with different N/P ratio was loaded onto a 1.2 % agarose gel containing 0.1% ethidium bromide and run for 10 min and taken to UV transilluminator for visualizing the bands.

RNase A protection assay

siRNA dendriplexes were incubated with 0.01 µg/µl RNase A for different periods of time at 37^{o}C and then treated with 0.2% SDS solution at 4^{o}C to release siRNA. Samples were then run in a 1.2% ethidium bromide containing agarose gel and taken to UV transilluminator for visualization of the bands. Naked siRNA served as a control.

Transmission electronic microscopic (TEM) imaging

A solution (0.5 mL) of siRNA (2 µM) was mixed with a solution (0.5 mL) of G6 (4.6 µM) dendrimer in D.I water at N/P ratio of 10. After 30 min equilibration at 37 ^{o}C, this mixture (1 mL) was dropped on a standard carbon-coated copper TEM grid and air-dried (1 h at 37^{o}C, ambient pressure). In the case of siRNA/dendrimer solutions, the samples were premixed and allowed to equilibrate for 30 min at 37^{o}C before placing on the grid. The grid was then stained with uranyl acetate (2% in 50% alcoholic solution) for 5 seconds, and the excess uranyl acetate was removed by filter paper. The dried specimens were observed with a JEOL 2010 transmission electron microscope operating at 200 kV. Data were analyzed with Digital Micrograph software.

Dynamic light scattering (DLS) analysis

The siRNA solution was mixed with indicated amount of amphiphilic dendrimer solution at N/P ratio 10. The final concentration of the siRNA was 1 μM. After incubated at 37 °C for 30 min, size distribution and zeta potential measurement was performed using Zetasizer Nano-ZS (Malvern, Ltd. Malvern, UK) with a He-Ne ion laser of 633 nm.

Cell culture and siRNA transfection

The human ovarian carcinoma cell line SKOV-3 was a gift from Dr. N. Auersperg (University of British Columbia, Vancouver, B. C., Canada), and cultured in Medium 199:MCDB 105 (1:1) (Sigma, St. Louis, MO) with 5% fetal bovine serum (Hyclone, Logan, UT) and 1% penicillin-streptomycin mixture (Invitrogen, Carlsbad, CA). SKOV-3 CSCs and HEYA8 CSCs were isolated, cultured and characterized as described[46]. Briefly, 5,000 cells/ml cells were seeded in ultra-low-attachment 100 mm culture dish in serum-free medium and nonadherent spherical clusters were selected by repeated culture for 8 to 10 passages. Each sphere was about 100 μm in diameter containing about 500-1,000 cells. Primary human peritoneal mesothelial cells obtained from patients undergoing surgery for benign conditions were isolated and cultured at 37°C for 2-3 days until a monolayer of polygonal cells had grown[22,47]. Ovarian surface epithelial (OSE) cells were obtained from normal ovaries from patients without malignant gynecological diseases and cultured as described[48]. For transfection, siRNA dendriplexes were prepared by diluting appropriate amounts of siRNA and G_6 dendrimer in the indicated solutions and incubated at room temperature for 30 min. Spheres or cells were then treated with siRNA dendriplexes for the indicated time.

Western blotting

Cells and tumors were collected and lysed using RIPA solution (1% Triton X-100, 50 mmol/l Tris-HCl; pH 7.4, 0.1% SDS, 150 mmol/l NaCl, and 5 mmol/l EDTA) supplemented with protease inhibitors (1 μg/ml aprotinin, 1 μg/ml leupeptin, 1 μg/ml pepstatin A, 1 mM phenylmethyl sulfonyl fluoride, 1 mM sodium orthovanadate and 1 mM sodium fluoride) and quantified using a DC protein assay kit (Bio-Rad, Hercules, CA). Equal amounts of protein (20 μg) were separated on 10% SDS-polyacrylamide gels and transferred to nitrocellulose membrane. Membranes were then blocked in 5% skim milk in PBS-Tween 20 and probed with anti-$p70^{S6K}$ (1:1,000) (Cell Signaling, Beverley, MA) and anti-β-actin (1:2,000) (Sigma, St Louis, MO) at 4°C overnight. Then membranes were then incubated with HRP-conjugated anti-rabbit secondary antibodies (1:5,000) (Bio-Rad, Hercules, CA). Western blot membranes were visualized using an enhanced chemiluminescent substrate (Perkin-Elmer, Waltham, MA) for detection of horseradish peroxidase (GE Healthcare, Little Chalfont, UK).

Reverse transcription-polymerase chain reaction (RT-PCR)

CSCs were transfected with siRNA/G6 complex and form spheres. Total RNA was isolated using Trizol (Invitrogen) according to the manufacturer's instructions. cDNA was synthesized using a First-strand cDNA synthesis kit (Invitrogen). PCR was performed with a set of primers: Bmi-1: sense 5'-ATGTGTGTGCTTTGTGGAG-3', anti-sense 5'-AGTGGTCTGGTCTTGTGAAC-3'; Nanog: sense 5'-AAGACAAG GTCCCGGTCAAG-3', antisense 5'-CCTAGTGGTCTGCTGTATTAC-3'; Oct4: sense 5'-ATCCTGGGGGTTCTATTTGG-3', antisense 5'-TCTCCAGGTTGCCT CTCACT-3'; and β-actin, sense 5'-TCACCGAGGCCCCTCTGAACCCTA-3', anti-sense 5'-GGCAGTAATCTCCTTCTGCATCCT-3'. β-actin served as a control.

MTT assay

Cells were incubated with MTT (0.5 mg/ml) solution at 37^{o}C for 2 h. The medium was removed and cells were diluted in DMSO. The colorimetric absorbance was read using Bio-Rad 550 microplate reader at 570 nm.

Sphere formation assay

5,000 cells/ml cells were seeded in ultra-low-attachment 100 mm culturing dish in serum-free medium. Pictures were taken every day for a week and the number of spheres was counted. For relapse (regrowth) experiments, CSCs were dissociated and re-plated to analyze in serial passage for secondary sphere formation. The number of spheres formed will be counted under a Nikon light microscope and photos will be acquired daily. Spheres were counted when they were ≥ 100 μm in diameter.

Migration and invasion assays

Twenty-four-well transwell filters (8 μm pore size) coated without or with 1 mg/ml Matrigel (50 μl/well, BD sciences, Mississauga, ON, Canada) were used to assess cell migration and invasion capability, respectively. Cells in serum-free medium were seeded in triplicate in the upper filter and medium containing 10% FBS was added to the lower wells. The chambers were incubated for 24 h at 37^{o}C. The cells that did not penetrate the filter were removed. The migrated/invaded cells on the lower surface of the filter were fixed with ice-cold methanol, stained with 0.5% crystal violet for 10 min, and counted under the microscope.

Cell adhesion assay

CSCs transfected with siRNA dendriplexes were labeled with fluorescence (H-1000, vector laboratories, Burlingame, CA) and overlaid onto a monolayer of confluent primary human mesothelial cells coated on a 24-wells plate and allowed to attach for 30 min. After removing non-adherent SKOV-3 CSCs, the adherent spheres were fixed and counted. The percentage of adhered spheres was calculated by dividing the number of spheres adhering on the mesothelium by the total number of spheres in each well before washing.

***In vivo* study**

Female athymic nude mice (5-6 weeks) were purchased from Charles River Laboratories (Wilmington, MA) and were cared for according to guidelines set forth by the University of Hong Kong. 10^6 SKOV-3 CSCs were subcutaneously injected into the right flank of the nude mice. Tumor volumes were calculated using the formula $(\pi/6)lw^2$, where l is the larger measurement and w is the smaller measurement. When tumors reached about 25 mm^3, 2.5 mg/kg siRNA/G_6 dendriplexes (N/P ratio = 10) were injected via the tail vein (n=3 per group, repeated twice). The injection was performed twice a week for one week. NS siRNA/G_6 dendriplexes were used as the control. Tumor size and body weight were measured for one week, and the mice were sacrificed by cervical dislocation. The tumors and organs were then excised. The collected tumors were fixed in formalin for paraffin embedding and tested for Ki67 and $p70^{S6K}$ expression by immunohistochemistry. Data are presented as mean ± SEM. Protein and RNA were also collected from the harvested tissues by the same method described above. The expression of $p70^{S6K}$ and stem cell markers (Bmi-1, Nanog, and Oct4) was measured by western blotting and RT-PCR as described above.

In vivo biodistribution study

Cy5- $p70^{S6K}$ siRNA/G_6 dendriplexes were injected via the tail vein into mice bearing tumors. PBS and naked Cy5- $p70^{S6K}$ siRNA were used as controls. Fluorescent images were taken after 0 min, 5 min, 30 min, 1 h, 2 h, 4 h, and 24 h of injection. The mice were harvested after 24 h of injection. Organs were collected and fluorescent images were also taken.

In vivo intraperitoneal metastasis study

10^6 SKOV-3 CSCs were injected intraperitoneally into the peritoneal cavity of mice (n=5 per group). 2.5 mg/kg siRNA/G_6 dendriplexes (N/P ratio = 10) were injected via the tail vein. The injection was performed twice a week for three weeks. NS siRNA/G_6 dendriplexes were used as the control. The mice were sacrificed and the number of disseminated tumor nodaules within the peritoneal cavity was counted. The volume of malignant ascites was also measured.

Statistical tests

All data are presented as mean ± SD unless otherwise indicated. Data derived from more than two groups were compared by one-way ANOVA followed by a Tukey's test. Data derived from two groups were compared by unpaired Student's *t* test. Differences were considered as statistically significant when the *P* value was less than 0.05.

Acknowledgements

Financial support from RGC Theme-based Research T12-401/13-R (ASTW), La Ligue contre Le Cancer (LP), Agence National de la Recherche in the framework of EuroNanoMed program for "DENANORNA", "Target4cancer" and "NANOGLIO" (LP), Fondation pour la Recherche Médicale (SPF20150934261 for YC and

SPF20160936294 for YJ), is gratefully acknowledged.

Figure Legends

Figure 1. (A) Schematic presentation of dendrimer-mediated siRNA delivery. (B) Chemical structure of the TEA-core PAMAM dendrimer (generation 3 is shown for the sake of simplicity).

Figure 2. Characterization of $p70^{S6K}$ siRNA/G_6 dendriplexes. (A) The ability of the G_6 dendrimer to bind with $p70^{S6K}$ siRNA (0.15 μg) in DEPC-treated water at different N/P ratios varying from 0 to 20 was tested using agarose gel electrophoresis. Naked $p70^{S6K}$ siRNA was used as the control (N/P ratio = 0). (B) Transmission electronic microscopy (TEM) imaging of $p70^{S6K}$ siRNA/G_6 dendriplexes at an N/P ratio of 10. (C) Dynamic light scattering (DLS, left) and zeta potential analysis (right) of $p70^{S6K}$ siRNA/G_6 dendriplexes at an N/P ratio of 10. (D) siRNA without (left) and with (right) G_6 was incubated with 0.01 μg/μl RNase A at room temperature for 30 min, and then with 0.2% SDS at 4°C. siRNA was analyzed by agarose gel electrophoresis.

Figure 3. $p70^{S6K}$ siRNA/G_6 dendriplex-mediated gene silencing and inhibition of cell viability of ovarian SKOV-3 CSCs, HEYA8 CSCs, and SKOV-3 non-CSCs without adverse toxicity to normal human ovarian surface epithelial cells (OSEs). $p70^{S6K}$ protein levels of (A, B) SKOV-3 CSCs, (D) SKOV-3 non-CSCs and (F) HEYA8 CSCs were measured after transfection with indicated solutions for 72 h. Viability of (C) SKOV-3 CSCs, (E) SKOV-3 non-CSCs and (G) HEYA8 CSCs was measured using MTT assay after treatment with indicated solutions. (H) Normal human OSEs were transfected with 20 nM $p70^{S6K}$ siRNA/G_6 or nonspecific NS siRNA/G_6 dendriplexes for the indicated time. $p70^{S6K}$ protein levels were measured using Western blot and quantified with β-actin as the control Cell viability was measured using MTT assay.

Data are presented as mean ± SD. *, $P < 0.05$ vs. NS siRNA/G_6.

Figure 4. $p70^{S6K}$ siRNA dendriplexes suppress CSC marker expression and secondary sphere formation. SKOV-3 CSCs were treated with $p70^{S6K}$ siRNA/G_6 or nonspecific NS siRNA/G_6 dendriplexes. (A) Expression of the stem cell markers Bmi-1, Nanog, and Oct4 were analysed using RT-PCR with specific primers. β-actin served as a control. (B) Bright-field pictures of CSCs were taken every day and the number of secondary spheres was counted. Bar represents 100 μm. Data are presented as mean ± SD. *, $P < 0.05$ vs. NS siRNA/G_6.

Figure 5. $p70^{S6K}$ siRNA dendriplexes inhibit (A) CSC-mesothelial interaction, (B) CSC migration and (C) invasion. (A) SKOV-3 CSCs transfected with 20 nM $p70^{S6K}$ siRNA/G_6 dendriplexes or nonspecific NS siRNA/G_6 were plated onto a confluent human peritoneal mesothelium monolayer and allowed to adhere for 30 min. After non-adherent CSCs were removed, the adherent CSCs were fixed and counted. SKOV-3 CSCs were treated with $p70^{S6K}$ siRNA/G_6 or NS siRNA/G_6 dendriplexes for 48 h and seeded in (B) non-coated and (C) Matrigel-coated transwell inserts for 24 h to assess migration and invasion, respectively. Cells in the upper chamber were removed after fixation. The remaining cells were stained with 0.5% crystal violet for 10 min. The number of (B) migrating or (C) invading cells were counted. Data are presented as mean ± SD. *, $P < 0.05$ vs. NS siRNA/G_6.

Figure 6. Mice with subcutaneous tumors derived from SKOV-3 CSCs were treated with i.v. injection of PBS, Cy5-$p70^{S6K}$ siRNA, or Cy5-$p70^{S6K}$ siRNA/G_6. (A) Comparison of fluorescence of mice after 0 min, 5 min, 30 min, 1 h, 2 h, 4 h, and 24 h

of injection. (B) Comparison of fluorescence in organs.

Figure 7. Mice with subcutaneous tumors derived from SKOV-3 CSCs were treated with intravenous injection of $p70^{S6K}$ siRNA/G_6 or nonspecific NS siRNA/G_6 as indicated for 1 week (siRNA dosage: 2.5 mg/kg, N/P ratio=10). (A) Comparison of treated mice and isolated tumors. (B) Tumor volumes were measured by calipers and recorded. (C) Immunohistochemistry staining of $p70^{S6K}$ and Ki67 in isolated tumors (200 x magnification). (D) Western blot analysis of the expression of $p70^{S6K}$ in tumors. (E) RT-PCR analysis of the expression of stem cell markers (Bmi-1, Nanog, and Oct4) in tumors. (F) Immunohistochemistry staining of CD133 in isolated tumors (200 x magnification). (G) Mouse body weight recording. (H) Comparison of livers from treated mice. (I) Blood biochemistry of alanine transaminase (ALT) and aspartate aminotransferase (AST) were measured using peripheral blood collected from retro-orbital sinus. Data are expressed as mean ±SEM (n=3, repeated twice). Bar=5 mm. An asterisk (*) indicates P <0.05 vs NS siRNA/G_6.

Figure 8. Mice were injected intraperitoneally with 10^6 SKOV-3 CSCs and treated with i.v. injected of $p70^{S6K}$ siRNA/G_6 or nonspecific NS siRNA/G_6 as indicated for 3 week (siRNA dosage: 2.5 mg/kg, N/P ratio=10). (A) Representative views of the metastases in the peritoneal cavity are shown. (B) The number of metastatic nodules were counted, and (C) ascites volume was collected and measured. (D) The number of survival mice were monitored during the treatment. Data are expressed as mean ±SD. An asterisk *, indicates P <0.05 vs NS siRNA/G_6.

References :

1. Mehlen, P., Puisieux, A. (2006). Metastasis: a question of life or death. Nat Rev Cancer **6**: 449-458.

2. Steeg, P. S. (2016). Targeting metastasis. Nat Rev Cancer **16**: 201-218.

3. Miller, K.D., Siegel, R.L., Lin, C.C., Mariotto, A.B., Kramer, J.L., Rowland, J.H., *et al*. (2016). Cancer treatment and survivorship statistics, 2016. CA Cancer J Clin **66**: 271-289.

4. Lapidot, T., Sirard, C., Vormoor, J., Murdoch, B., Hoang, T., Caceres-Cortes, J., *et al*. (1994). A cell initiating human acute myeloid leukaemia after transplantation into SCID mice. Nature **367**: 645-648.

5. Liao, W.T., Ye, Y.P., Deng, Y.J., Bian, X.W., Ding, Y.Q. (2014). Metastatic cancer stem cells: from the concept to therapeutics. Am J Stem Cells **3**: 46-62.

6. Liu, S., Ye, D., Guo, W., Yu, W., He, Y., Hu, J., *et al*. (2015). G9a is essential for EMT-mediated metastasis and maintenance of cancer stem cell-like characters in head and neck squamous cell carcinoma. Oncotarget **6:** 6887-6901.

7. Leth-Larsen, R., Terp, M.G., Christensen, A.G., Elias, D., Kühlwein, T., Jensen, O.N., *et al*. (2012). Functional heterogeneity within the CD44 high human breast cancer stem cell-like compartment reveals a gene signature predictive of distant metastasis. Mol Med **18**: 1109-1121.

8. Nassar, D., Blanpain, C. (2016). Cancer stem cells: basic concepts and therapeutic implications. Annu Rev Pathol-Mech **11**: 47-76.

9. Campbell, I.G., Russell, S.E., Choong, D.Y.H., Montgomery, K.G., Ciavarella, M.L.,

Hooi, C.S.F., *et al*. (2004). Mutation of the PIK3CA gene in ovarian and breast cancer. Cancer Res **64**: 7678-7681.

10. Pon, Y.L., Zhou, H.Y., Cheung, A.N.Y., Ngan, H.Y.S., Wong, A.S.T. (2008). p70 S6 kinase promotes epithelial to mesenchymal transition through snail induction in ovarian cancer cells. Cancer Res **68**: 6524-6532.

11. Ip, C.K.M., Yung, S., Chan, T.M., Tsao, S.W., Wong, A.S.T. (2014). p70 S6 kinase drives ovarian cancer metastasis through multicellular spheroid-peritoneum interaction and P-cadherin/b1 integrin signaling activation. Oncotarget **5:** 9133-9149.

12. Zhou, H.Y., Wong, A.S.T. (2006). Activation of p70S6K induces expression of matrix metalloproteinase 9 associated with hepatocyte growth factor-mediated invasion in human ovarian cancer cells. Endocrinology **147**: 2557-2566.

13. Lam, S.S.N., Ip, C.K.M., Mak, A.S.C., Wong, A.S.T. (2016). A novel p70 S6 kinase-microRNA biogenesis axis mediates multicellular spheroid formation in ovarian cancer progression. Oncotarget **7:** 38064-38077.

14. Imai, K., Takaoka, A. (2006). Comparing antibody and small-molecule therapies for cancer. Nat Rev Cancer **6**: 714-727.

15. Leng, T.D., Xiong, Z.G. (2013). The pharmacology and therapeutic potential of small molecule inhibitors of acid-sensing ion channels in stroke intervention. Acta Pharmacol Sin **34**: 33-38.

16. Wittrup, A., Lieberman, J. (2015). Knocking down disease: a progress report on siRNA therapeutics. Nat Rev Genet **16**: 543-552.

17. Kanasty, R., Dorkin, J.R., Vegas, A., Anderson, D. (2013). Delivery materials for

siRNA therapeutics. Nat Mater **12**: 967-977.

18. Tseng, Y.C., Mozumdar, S., Huang, L. (2009). Lipid-based systemic delivery of siRNA. Adv Drug Deliv Rev **61**: 721-731.

19. Schroeder, A., Levins, C.G., Cortez, C., Langer, R., Anderson, D.G. (2010). Lipid-based nanotherapeutics for siRNA delivery. J Intern Med **267**: 9-21.

20. Wagner, E. (2012). Polymers for siRNA delivery: inspired by viruses to be targeted, dynamic, and precise. Acc Chem Res **45**: 1005-1013.

21. Liu, X., Rocchi, P., Peng, L. (2012). Dendrimers as non-viral vectors for siRNA delivery. New J Chem **36**: 256-263.

22. Liu, X., Liu, C., Catapano, C.V., Peng, L., Zhou, J., Rocchi, P. (2014). Structurally flexible triethanolamine-core poly(amidoamine) dendrimers as effective nanovectors to deliver RNAi-based therapeutics. Biotechnol Adv **32**: 844-852.

23. Zhou, J., Wu, J., Hafdi, N., Behr, J.P., Erbacher, P., Peng, L. (2006). PAMAM dendrimers for efficient siRNA delivery and potent gene silencing. Chem Commun: 2362-2364.

24. Wu, J., Zhou, J., Qu, F., Bao, P., Zhang, Y., Peng, L. (2005). Polycationic dendrimers interact with RNA molecules: polyamine dendrimers inhibit the catalytic activity of Candida ribozymes. Chem Commun: 313-315.

25. Cui, Q., Yang, S., Ye, P., Tian, E., Sun, G., Zhou, J., *et al.* (2016). Downregulation of TLX induces TET3 expression and inhibits glioblastoma stem cell self-renewal and tumorigenesis. Nat Commun **7**: 10637.

26. Reebye, V., Sætrom, P., Mintz, P.J., Huang, K.W., Swiderski, P., Peng, L., *et al.*

(2014). Novel RNA oligonucleotide improves liver function and inhibits liver carcinogenesis in vivo. Hepatology **59**: 216-227.

27. Kala, S., Mak, A.S.C., Liu, X., Posocco, P., Pricl, S., Peng, L., *et al*. (2014). Combination of dendrimer-nanovector-mediated small interfering RNA delivery to target Akt with the clinical anticancer drug paclitaxel for effective and potent anticancer activity in treating ovarian cancer. J Med Chem **57**: 2634-2642.

28. Liu, X., Liu, C., Chen, C., Bentobji, M., Cheillan, F.A., Piana, J.T., *et al*. (2014). Targeted delivery of Dicer-substrate siRNAs using a dual targeting peptide decorated dendrimer delivery system. Nanomedicine **10**: 1627-1636.

29. Zhou, J., Neff, C.P., Liu, X., Zhang, J., Li, H., Smith, D.D., *et al.* (2011). Systemic administration of combinatorial dsiRNAs via nanoparticles efficiently suppresses HIV-1 infection in humanized mice. Mol Ther **19**: 2228-2238.

30. Wei, T., Chen, C., Liu, J., Liu, C., Posocco, P., Liu, X., *et al.* (2016). Anticancer drug nanomicelles formed by self-assembling amphiphilic dendrimer to combat cancer drug resistance. Proc Natl Acad Sci U S A **112**: 2978-2983.

31. Chen, C., Posocco, P., Liu, X., Cheng, Q., Laurini, E., Zhou, J., *et al.* (2016). Mastering dendrimer self-assembly for efficient siRNA delivery: from conceptual design to in vivo efficient gene silencing. Small **12**: 3667-3676.

32. Liu, X., Wang, Y., Chen, C., Tintaru, A., Cao, Y., Liu, J., et al. (2016). A fluorinated bola-amphiphilic dendrimer for on-demand delivery of siRNA via specific response to reactive oxygen species. Adv Funct Mater 26: 8594-8603.

33. Matsumura, Y., Maeda, H. (1986). A new concept for macromolecular therapeutics

in cancer chemotherapy: mechanism of tumoritropic accumulation of proteins and the antitumor agent smancs. Cancer Res. **46**: 6387-6392.

34. Chauhan, V.P., Jain, R.K. (2013). Strategies for advancing cancer nanomedicine.Nat. Mater. **12**: 958-962.

35. Chau, W.K., Ip, C.K., Mak, A.S.C., Lai, H.C., Wong, A.S.T. (2013). c-Kit mediates chemoresistance and tumor-initiating capacity of ovarian cancer cells through activation of Wnt/β-catenin-ATP-binding cassette G2 signaling. Oncogene **32**: 2767-2781.

36. Ip, C.K., Wong, A.S. (2012). Exploiting p70 S6 kinase as a target for ovarian cancer. Expert Opin. Ther. Targets **16:** 619-630.

37. Lengyel, E. (2010). Ovarian Cancer Development and Metastasis. Am J Pathol **177**: 1053-1064.

38. Davidowitz, R.A., Iwanicki, M.P., Brugge, J.S. (2012). In vitro mesothelial clearance assay that models the early steps of ovarian cancer metastasis. J Vis Exp: 3888.

39. Kim, J.E., Chen, J. (2000). Cytoplasmic-nuclear shuttling of FKBP12-rapamycin-associated protein is involved in rapamycin-sensitive signaling and translation initiation. Proc Natl Acad Sci U S A. **97**: 14340-14345.

40. Valovka, T., Verdier, F., Cramer, R., Zhyvoloup, A., Fenton, T., Rebholz, H. *et al.* (2003). Protein kinase C phosphorylates ribosomal protein S6 kinase betaII and regulates its subcellular localization. Mol Cell Biol **23**: 852-863.

41. Rosner, M., Hengstschlager, M. (2011). Nucleocytoplasmic localization of p70

S6K1, but not of its isoforms p85 and p31, is regulated by TSC2/mTOR. Oncogene **30**: 4509-4522.

42. de Groot, R.P., Ballou, M., Sassone-Corsi, P. (1994). Positive regulation of the cAMP-responsive activator CREM by the p70 S6 kinase: an alternative route to mitogen-induced gene expression. Cell **79**: 81-91

43. Fleckenstein, D.S., Dirks, W.G., Drexler, H.G., Quentmeier, H. (2003). Tumor necrosis factor receptor-associated factor (TRAF) 4 is a new binding partner for the p70S6 serine/threonine kinase. Leuk Res **27**: 687-694.

44. Liu, X., Wu, J., Yammine, M., Zhou, J., Posocco, P., Viel, S., *et al*. (2011). Structurally flexible triethanolamine core PAMAM dendrimers are effective nanovectors for DNA transfection in vitro and in vivo to the mouse thymus. Bioconjug Chem **22**: 2461-2473.

45. Kawano, K., Tsuda, N., Matsueda, S., Sasada, T., Watanabe, N., Ushijima, K., *et al.* (2014). Feasibility study of personalized peptide vaccination for recurrent ovarian cancer patients. Immunopharmacol Immunotoxicol **36**:224-236.

46. Iwanicki, M.P., Davidowitz, R.A., Ng, M.R., Besser, A., Muranen, T., Merritt, M., *et al.* (2011). Ovarian cancer spheroids use myosin-generated force to clear the mesothelium. Cancer Discov. **1**: 144-157.

47. Yung, S., Chen, X.R., Tsang, R.C., Zhang, Q., Chan, T.M. (2004). Reduction of perlecan synthesis and induction of TGF-β1 in human peritoneal mesothelial cells due to high dialysate glucose concentration: implication in peritoneal dialysis. J Am Soc Nephrol **15**: 1178-1188.

48. Chan, R.W.S., Mak, A.S.C., Yeung, W.S.B., Lee, K.F., Cheung, A.N.Y., Ngan, H.Y.S., *et al*. (2013). Human female reproductive tract epithelial cell culture. Methods Mol Biol **945**: 347-363.

Figure 1

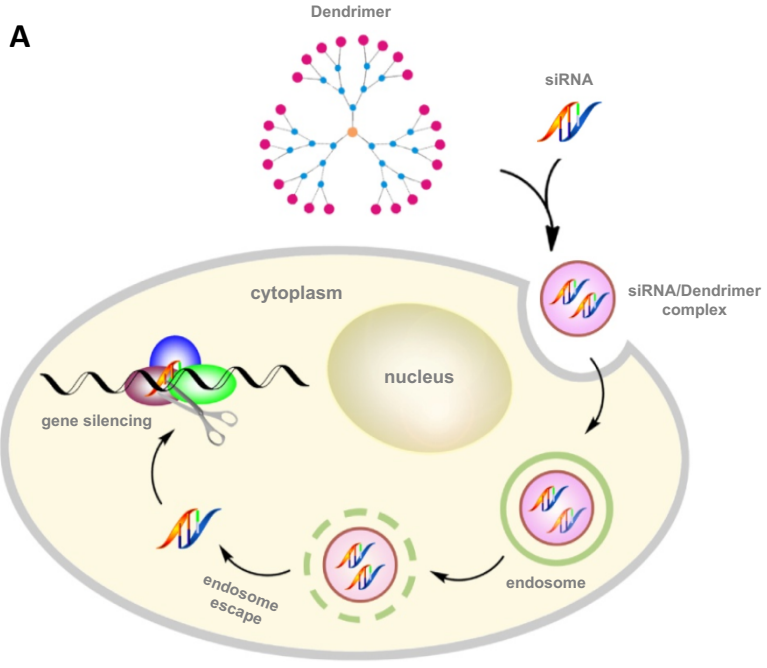
A
Dendrimer
siRNA
siRNA/Dendrimer
complex
cytoplasm
nucleus
gene silencing
endosome
endosome
escape

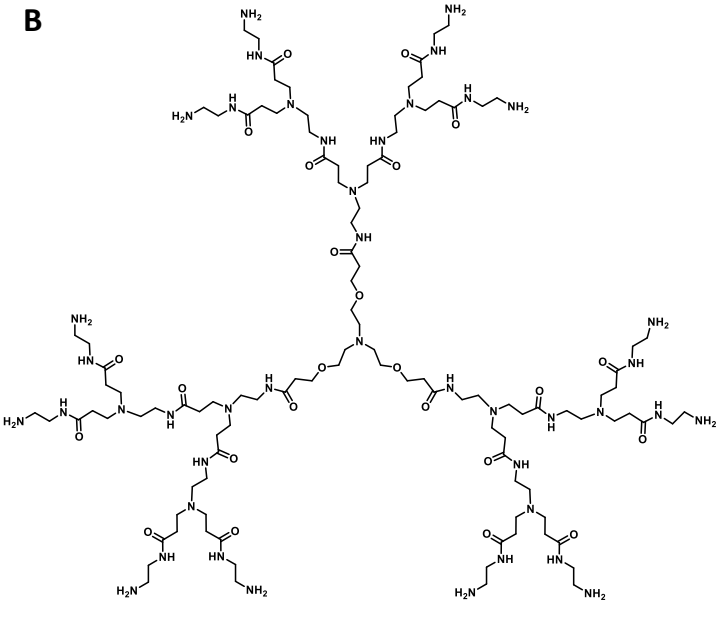
B

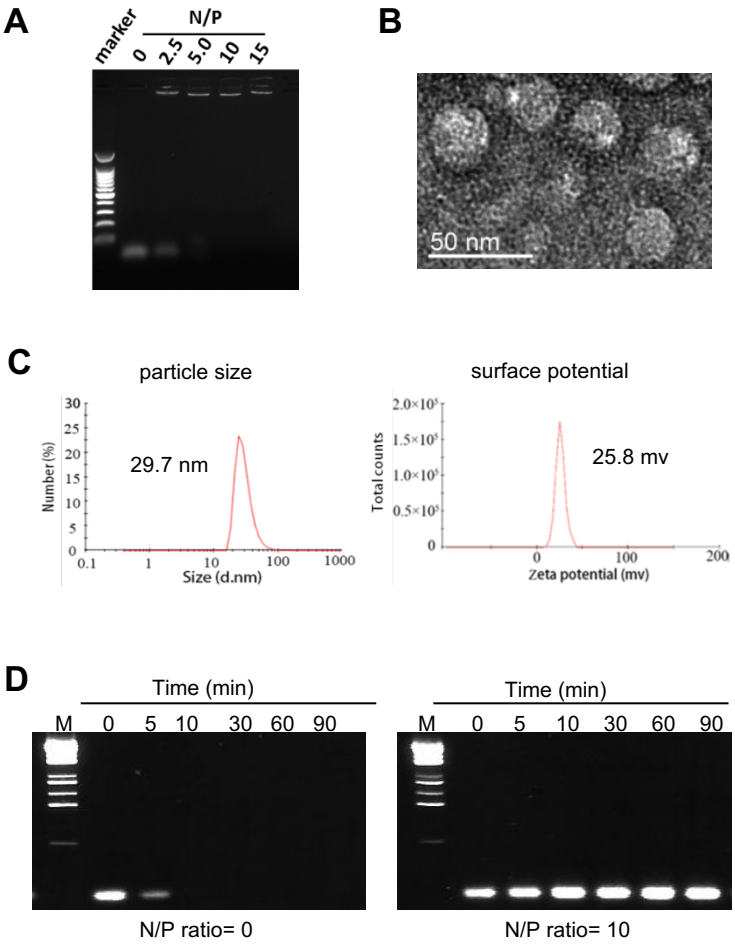
A
marker
N/P
0
2.5
5.0
10
15
B
50 nm
C
particle size
29.7 nm
Number (%)
Size (d.nm)
surface potential
25.8 mv
Total counts
Zeta potential (mv)
D
Time (min)
M
0
5
10
30
60
90
N/P ratio= 0
Time (min)
M
0
5
10
30
60
90
N/P ratio= 10

Figure 3

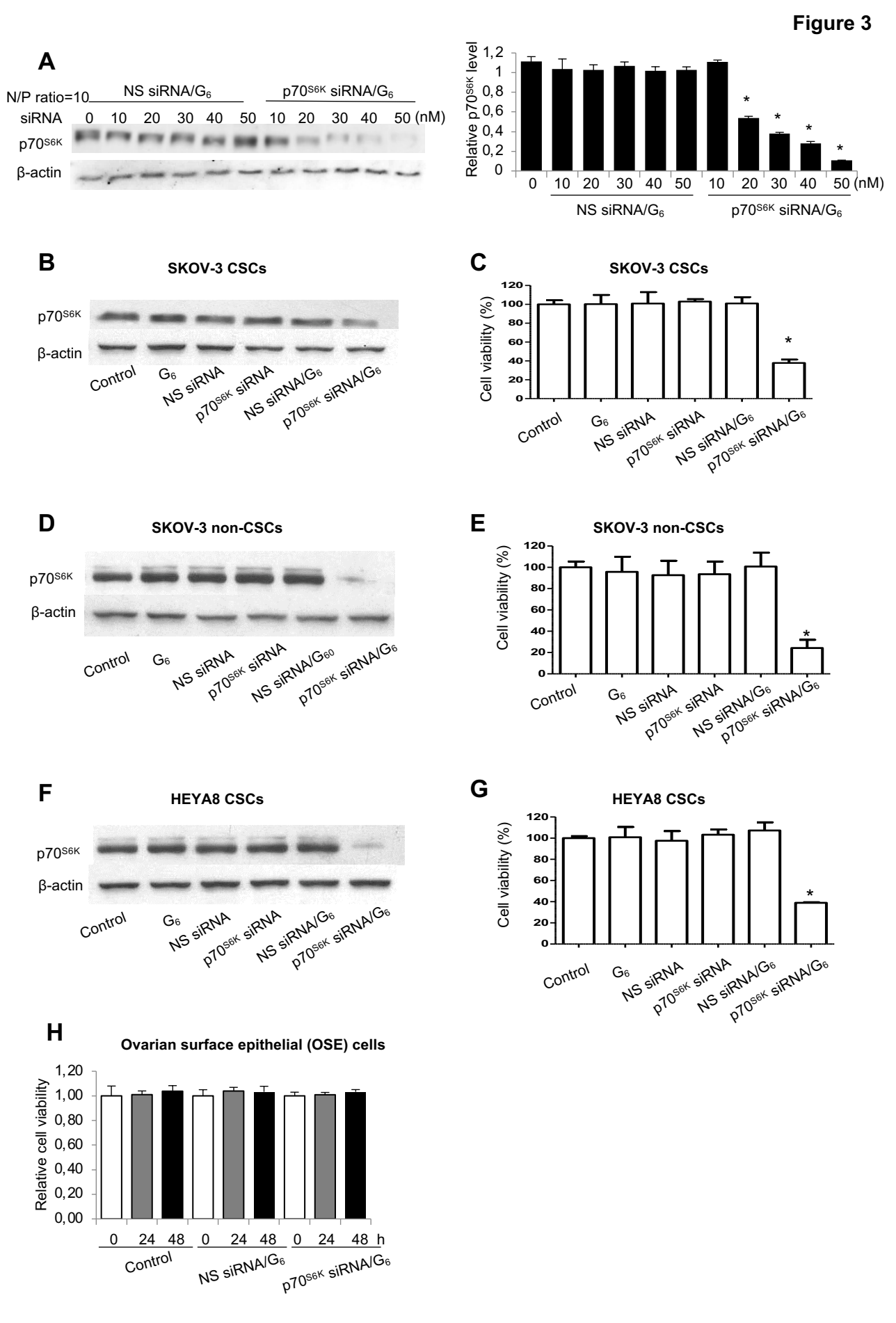
A
N/P ratio=10
NS siRNA/G6
p70S6K siRNA/G6
siRNA 0 10 20 30 40 50 10 20 30 40 50 (nM)
p70S6K
β-actin
Relative p70S6K level
1,2
1
0,8
0,6
0,4
0,2
0
0 10 20 30 40 50 10 20 30 40 50 (nM)
NS siRNA/G6
p70S6K siRNA/G6
B
SKOV-3 CSCs
p70S6K
β-actin
Control
G6
NS siRNA
p70S6K siRNA
NS siRNA/G6
p70S6K siRNA/G6
C
SKOV-3 CSCs
Cell viability (%)
120
100
80
60
40
20
0
Control
G6
NS siRNA
p70S6K siRNA
NS siRNA/G6
p70S6K siRNA/G6
D
SKOV-3 non-CSCs
p70S6K
β-actin
Control
G6
NS siRNA
p70S6K siRNA
NS siRNA/G60
p70S6K siRNA/G6
E
SKOV-3 non-CSCs
Cell viability (%)
120
100
80
60
40
20
0
Control
G6
NS siRNA
p70S6K siRNA
NS siRNA/G6
p70S6K siRNA/G6
F
HEYA8 CSCs
p70S6K
β-actin
Control
G6
NS siRNA
p70S6K siRNA
NS siRNA/G6
p70S6K siRNA/G6
G
HEYA8 CSCs
Cell viability (%)
120
100
80
60
40
20
0
Control
G6
NS siRNA
p70S6K siRNA
NS siRNA/G6
p70S6K siRNA/G6
H
Ovarian surface epithelial (OSE) cells
Relative cell viability
1,20
1,00
0,80
0,60
0,40
0,20
0,00
0 24 48 0 24 48 0 24 48 h
Control
NS siRNA/G6
p70S6K siRNA/G6

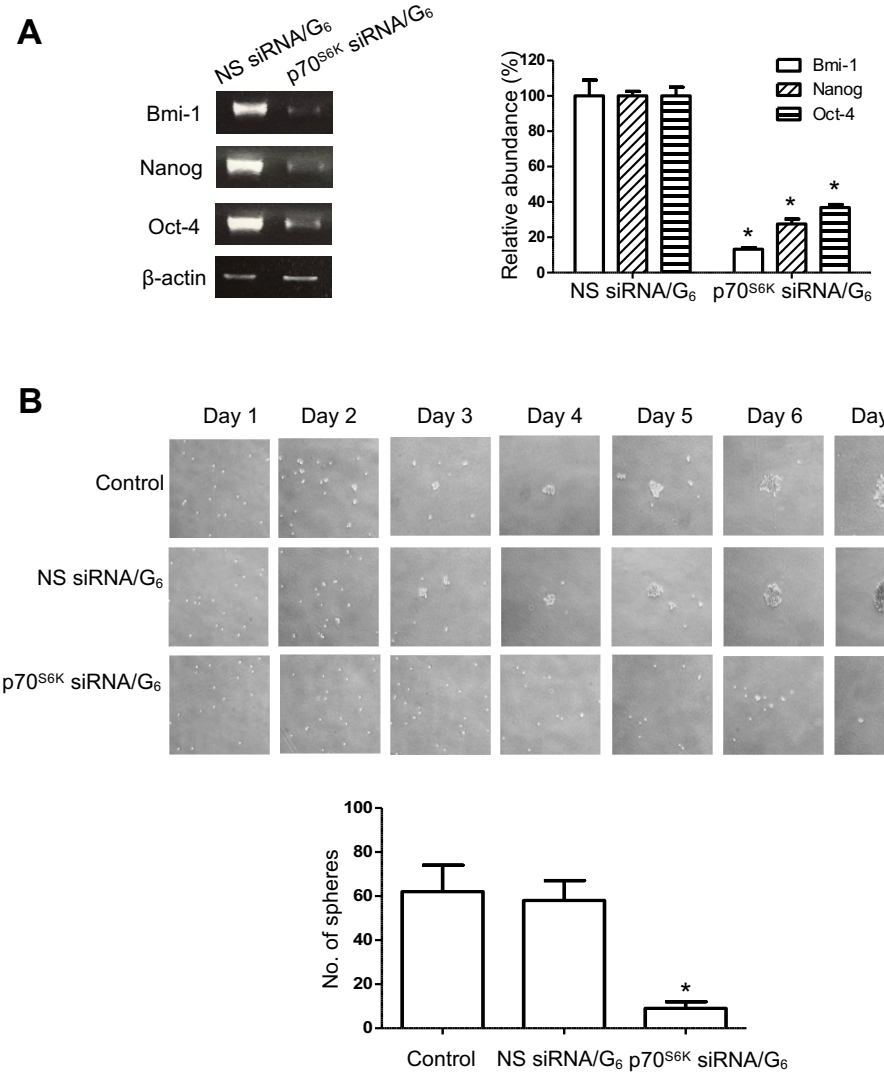
A
NS siRNA/G6
p70S6K siRNA/G6
Bmi-1
Nanog
Oct-4
β-actin
Relative abundance (%)
120
100
80
60
40
20
0
Bmi-1
Nanog
Oct-4
*
*
*
NS siRNA/G6
p70S6K siRNA/G6
B
Day 1
Day 2
Day 3
Day 4
Day 5
Day 6
Day 7
Control
NS siRNA/G6
p70S6K siRNA/G6
No. of spheres
100
80
60
40
20
0
*
Control
NS siRNA/G6
p70S6K siRNA/G6

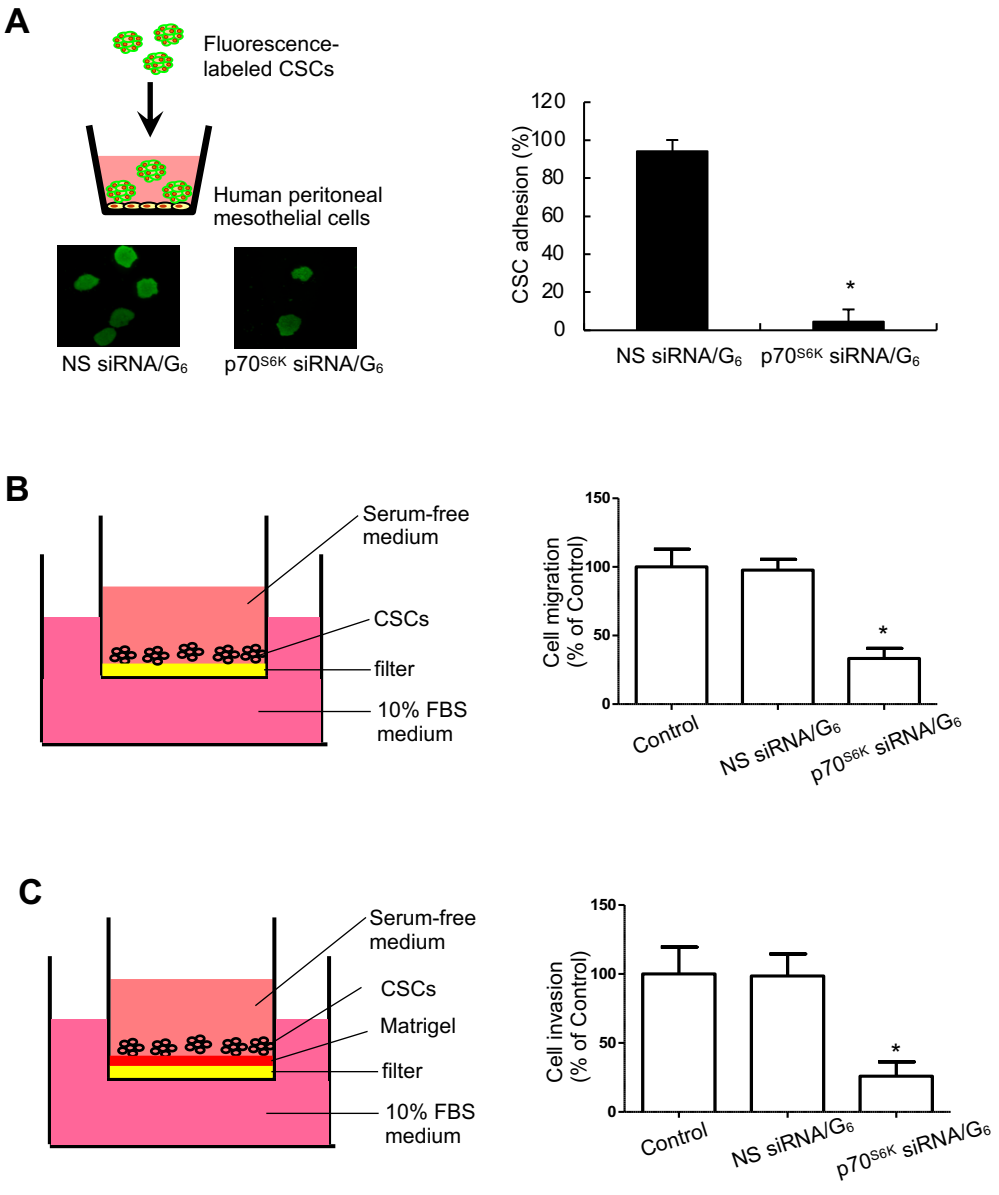
A
Fluorescence-labeled CSCs
Human peritoneal mesothelial cells
NS siRNA/G6
p70S6K siRNA/G6
CSC adhesion (%)
120
100
80
60
40
20
0
*
NS siRNA/G6
p70S6K siRNA/G6
B
Serum-free medium
CSCs
filter
10% FBS medium
Cell migration (% of Control)
150
100
50
0
*
Control
NS siRNA/G6
p70S6K siRNA/G6
C
Serum-free medium
CSCs
Matrigel
filter
10% FBS medium
Cell invasion (% of Control)
150
100
50
0
*
Control
NS siRNA/G6
p70S6K siRNA/G6

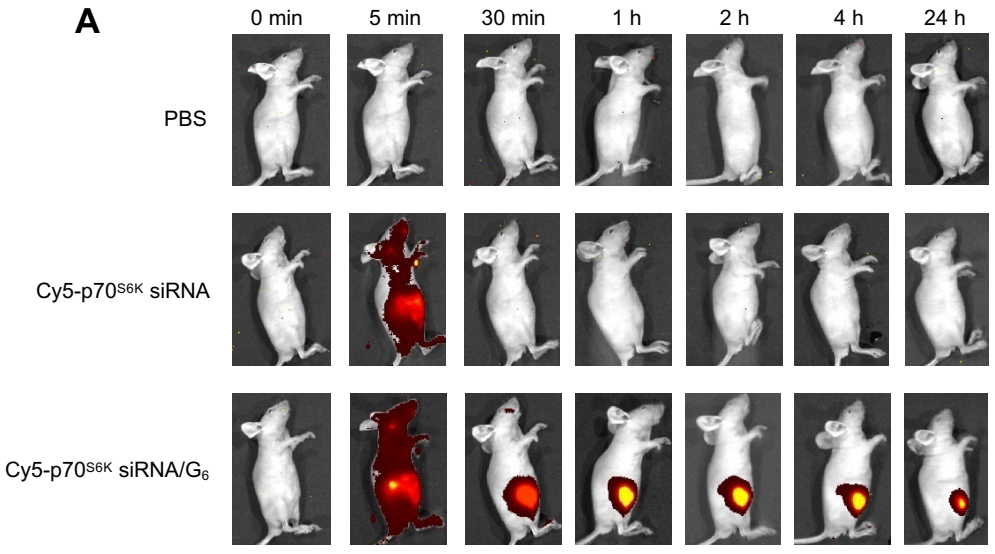
A
0 min
5 min
30 min
1 h
2 h
4 h
24 h
PBS
Cy5-p70S6K siRNA
Cy5-p70S6K siRNA/G6

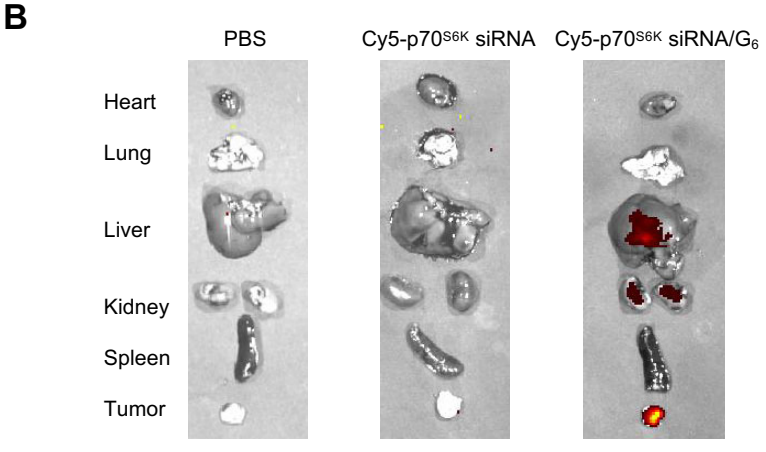
B
PBS
Cy5-p70S6K siRNA
Cy5-p70S6K siRNA/G6
Heart
Lung
Liver
Kidney
Spleen
Tumor

Figure 7

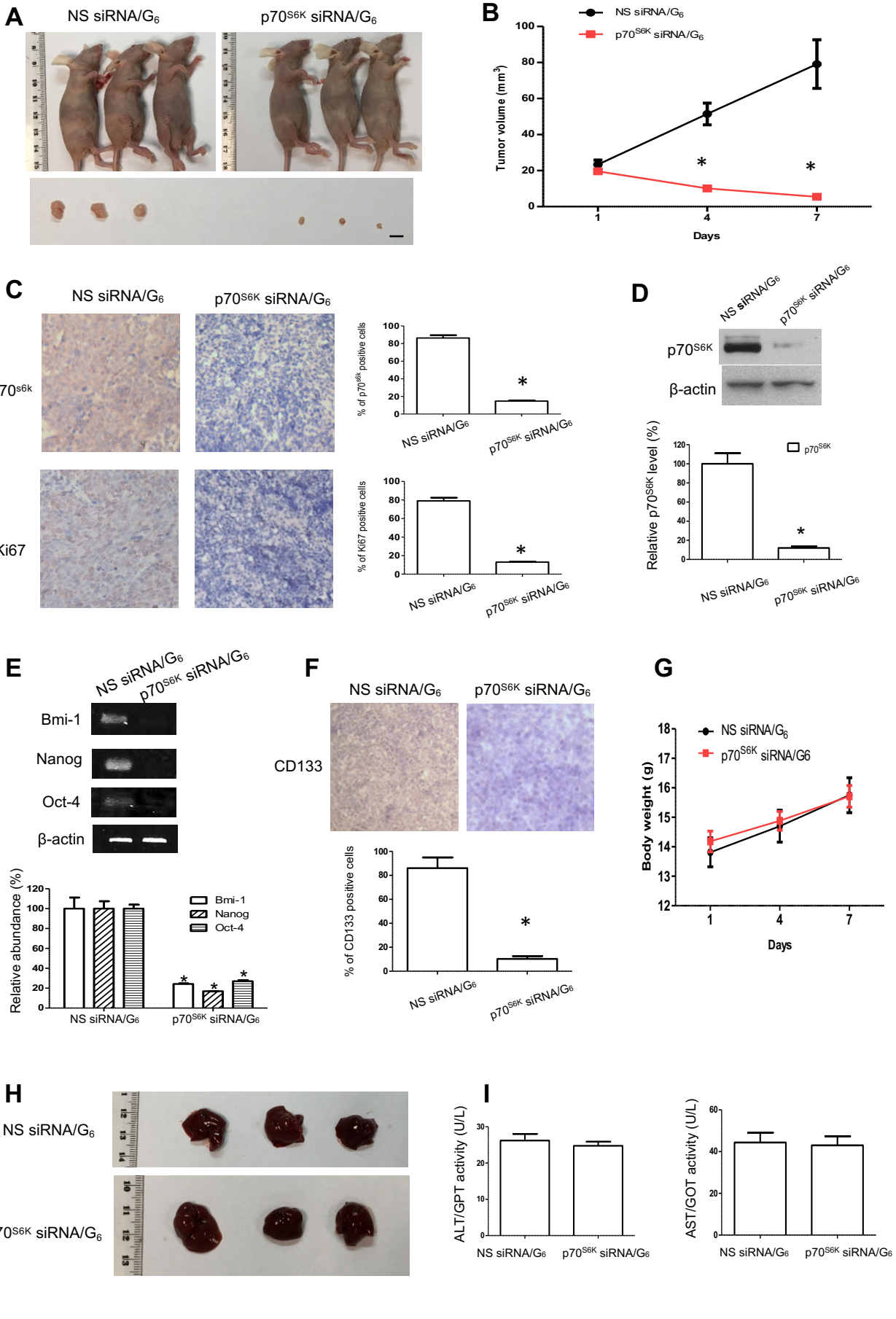
A
NS siRNA/G6
p70S6K siRNA/G6
B
NS siRNA/G6
p70S6K siRNA/G6
Tumor volume (mm3)
Days
C
NS siRNA/G6
p70S6K siRNA/G6
p70s6k
Ki67
% of p70s6k positive cells
% of Ki67 positive cells
D
p70S6K
β-actin
Relative p70S6K level (%)
E
Bmi-1
Nanog
Oct-4
β-actin
Relative abundance (%)
F
CD133
% of CD133 positive cells
G
Body weight (g)
Days
H
I
ALT/GPT activity (U/L)
AST/GOT activity (U/L)

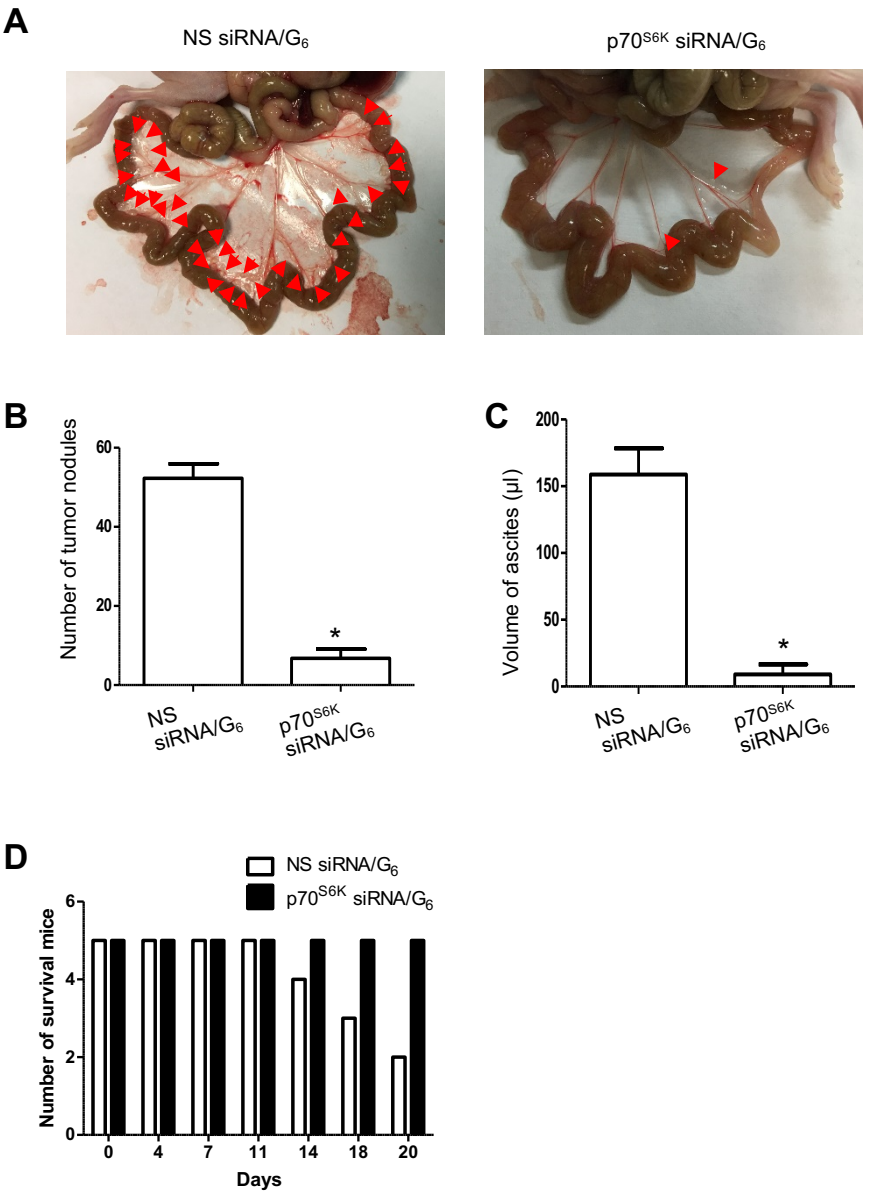
A
NS siRNA/G6
p70S6K siRNA/G6
B
Number of tumor nodules
60
40
20
0
*
NS siRNA/G6
p70S6K siRNA/G6
C
Volume of ascites (µl)
200
150
100
50
0
*
NS siRNA/G6
p70S6K siRNA/G6
D
NS siRNA/G6
p70S6K siRNA/G6
Number of survival mice
6
4
2
0
0
4
7
11
14
18
20
Days